

1966

The dynamic behavior of a single span prestressed concrete box-beam highway bridge, Report, C.E. 406, July 1966

R. F. Varney

Follow this and additional works at: <http://preserve.lehigh.edu/engr-civil-environmental-fritz-lab-reports>

Recommended Citation

Varney, R. F., "The dynamic behavior of a single span prestressed concrete box-beam highway bridge, Report, C.E. 406, July 1966" (1966). *Fritz Laboratory Reports*. Paper 230.
<http://preserve.lehigh.edu/engr-civil-environmental-fritz-lab-reports/230>

This Technical Report is brought to you for free and open access by the Civil and Environmental Engineering at Lehigh Preserve. It has been accepted for inclusion in Fritz Laboratory Reports by an authorized administrator of Lehigh Preserve. For more information, please contact preserve@lehigh.edu.

315.4 ST



C.E. 406

THE DYNAMIC BEHAVIOR
OF A SINGLE SPAN PRESTRESSED CONCRETE
BOX BEAM HIGHWAY

by
Robert F. Varney

FRITZ ENGINEERING
LABORATORY LIBRARY

A report submitted to the
Department of Civil Engineering

Fritz Engineering Laboratory Report No. 315.4 ST

RESEARCH INSTITUTE OF ENGINEERING AND TECHNOLOGY

Lehigh University

Department of Civil Engineering

CE 406

Report on

THE DYNAMIC BEHAVIOR
OF A SINGLE SPAN PRESTRESSED CONCRETE
BOX BEAM HIGHWAY BRIDGE

by

Robert F. Varney

THE DYNAMIC BEHAVIOR
OF A SINGLE SPAN PRESTRESSED CONCRETE
BOX BEAM HIGHWAY BRIDGE

Robert F. Varney

A report on an Investigation Sponsored by:

PENNSYLVANIA DEPARTMENT OF HIGHWAYS
U. S. DEPARTMENT OF COMMERCE
BUREAU OF PUBLIC ROADS

Fritz Engineering Laboratory
Department of Civil Engineering
Lehigh University
Bethlehem, Pennsylvania

July 1966

T A B L E O F C O N T E N T S

	Page
ABSTRACT	1
1. INTRODUCTION	3
2. DESCRIPTION OF TEST PROGRAM	6
2.1 Test Structure	6
2.2 Gages Used	8
2.3 Site Preparation	9
2.4 Test Vehicle	11
2.5 Test Procedure	12
2.6 Reduction of Records	14
3. TEST RESULTS	16
3.1 Deck Profile Smoothness	16
3.2 Bridge Response	17
4. DISCUSSION OF RESULTS	21
4.1 Beam Responses	21
4.2 Deck Slab Responses	26
4.3 Diaphragm Responses	30
4.4 Test Vehicle Responses	31
4.5 Directional Effect	32
4.6 Damping Effect	32

	Page
5. SUMMARY AND CONCLUSIONS	34
6. NOMENCLATURE	38
7. TABLES	39
8. FIGURES	57
9. ACKNOWLEDGMENTS	68
10. REFERENCES	69
11. BIBLIOGRAPHY	70

A B S T R A C T

This study covers the analysis of the dynamic strains and deflections obtained from extensive field measurements made on a full size single span prestressed concrete spread box beam highway bridge under controlled test vehicle loading. The test variables included vehicle placement, speed and direction.

The report contains an analysis of the dynamic amplifications of strain and deflection in comparison with the static live load responses at the same critical points on the structure for identical conditions of test vehicle placement and direction. A companion report prepared by others will investigate other aspects of the static live load behavior to which the findings of this study may relate.

It was found that the test bridge was more sensitive to impact loading than typical steel beam bridges of similar span lengths. The complex bridge-vehicle interaction which results in a wide range of dynamic amplifications was found to be essentially independent of the frequency of axle passage and of the initial position of the sprung load as the vehicle comes on the bridge. The bridge loaded frequency was found to be the best indicator of the relative magnitude of the dynamic amplification.

The bridge deck slab was found to be subject to live load strain reversals which may prove to be of significance in the search for a better understanding of highway bridge deck slab performance.

1. I N T R O D U C T I O N

This report documents the research techniques followed in carrying out a series of dynamic loading tests with a heavily loaded vehicle on a full size single span highway bridge and identifies, analyzes and interprets the various aspects of the dynamic behavior of the bridge under a sequence of controlled test vehicle loadings. The findings reported herein cover one phase of a comprehensive program of static and dynamic loadings of one of the types of prestressed concrete highway bridges currently used in Pennsylvania. This report concerns the dynamic behavior of the prestressed concrete spread box beam type which is being studied. A companion report being prepared by others deals with a more detailed examination of the static live load behavior of the same structure. This report provides a detailed analysis of the dynamic behavior of a specific structure through the media of strains and deflections recorded by gages mounted at critical locations. No attempt is made to develop an "impact factor" from the limited findings in the study of this single bridge. Rather, the emphasis has been placed on the detailed identification and interpretation of the various physical phenomena evident from the strain and deflection records.

As progress is made toward the development of an analytical method of predicting the dynamic behavior of highway bridges under moving loads to supplant present empirical methods, this report and others of a similar vein noted in the Bibliography will provide the definitive parameters for the mathematical model which can only be determined by such experimental studies. It is beyond the scope of this report to derive and compare theoretical predictions of dynamic response with the experimental data. A subsequent study toward this end is planned in collaboration with the author of an analytical computer program designed to correlate the findings of this and other completed field studies with the theoretical prediction of dynamic responses.

The dynamic behavior of a bridge study may be categorized in three ways: by dynamic amplifications of strains and deflections; by the fundamental frequencies of natural vibrations; and by the damping characteristics expressed as the logarithmic decrement of vibration. These values have been examined in relation to the four major elements of structural response with which this study is concerned: beam deflections, beam strains, deck slab strains and diaphragm strains.

Dynamic amplification has been determined relative to base values obtained from crawl speed tests for identical test vehicle paths. The crawl speed strains had been determined both for the report on the static live load effects and also as a base for dynamic analyses. This report involves the evaluation and analysis of the response of 19 gages on 51 high-speed runs along five test run paths at speeds from 10 mph to 42 mph. This report will complement the companion report on the static live load effects in that the latter report, among other findings, will develop a correlation of actual and theoretical response to static live loading. This report in turn examines the second phase of the total vehicular loading effect, that is, the dynamic amplification for the same live loading. In the detailing of significant characteristic phenomena of moving loads, vibration frequency variations and bridge damping characteristics, the material of this report is independent of any findings in the companion study.

2. DESCRIPTION OF TEST PROGRAM

The field study described herein was carried out during the period August 12-27, 1965 by a joint team of researchers comprised of four members from the U. S. Bureau of Public Roads Task Group for Bridge Research and five members from the Lehigh University Department of Civil Engineering. All elements of the research program were carried out by this team, including site preparation, gage installation and connection, operation of the electronic instrumentation and the test vehicle, recording of data and control of traffic. This field study was part of an extensive program of research carried out by this team on three related bridges at widely separated locations in Pennsylvania during the late summer of 1965.

2.1 TEST STRUCTURE

The data reported herein were taken on the center span of a three-span simply supported prestressed concrete spread box beam bridge carrying a secondary road designated L. R. 40091 over the westbound roadway of Interstate Highway 80 near Nescopeck, Pennsylvania. The test span is supported by four prestressed concrete hollow box beams 66 ft. 7 in. in length. The beam span is 65 ft. 3 in. and the lateral spacing is 8 ft. 9 3/8 in..

The bridge has a 28 ft. roadway (curb-to-curb) and is essentially symmetrical with a skew of just under 2° . The design called for a slab with 7 1/2 in. minimum thickness between beams. The test span is founded on spread footings and the beams are seated on elastomeric bearing pads. The pretensioned box beams were 48 in. wide and 39 in. deep in cross-section, with wall and base thicknesses of 5 in. and an upper surface thickness of 3 in.. The beams were interconnected at midspan by 10-in. thick diaphragms cast monolithically with the deck slab. An elevation of the structure, showing the cross-section 3.55 ft. north of midspan at which strain gages were located, is given in Fig. 1. This is the section at which maximum moment is produced by the test vehicle for north-bound runs. The bridge was generally oriented north-south on a 2.8% down grade to the north. There was an abrupt 90° turn in the roadway several hundred feet north of the bridge. The approach from the south was on a tangent well over 1000 ft. in length. A cross-section of the bridge shown in Fig. 2 indicates the center line of the paths followed by the test vehicle, and the specific location of the gages used. Three strain gages were located on the underside of the slab, three on the underside of the diaphragms, six on the underside of the beams and one on the top surface of the parapet. The beams are numbered 1 to 4 from east-to-west and the

test vehicle paths are numbered 1 to 5 east-to-west.

The bridge is of a type widely used in Pennsylvania and was designed in accordance with the design standards of the Pennsylvania Department of Highways.¹ These standards are primarily in line with the provisions of the AASHO Standard Specifications for Highway Bridges.² The bridge was designed for H20-S16-44 loading and had been completed and opened to traffic only a short time before the conduct of the test.

2.2 GAGES USED

The strain gages used for the dynamic analysis (Fig. 2) were chosen from a larger number of gages available because the preliminary analyses indicated that these gages provided the best measure of the dynamic response. The additional gages on the same section will be used to provide the detailed analysis of the static live load response of the structure which is covered in a companion report. All strain gages were of the bonded wire SR-4 type with 5-in. and 6-in. effective lengths.

The deflection gages which were designed by the Bureau of Public Roads were made of 1/8-in. thick aluminum plates tapered from 1 in. to 4 3/8 in. in width over a 12 in. length. Four strain gages were mounted near the wider end of each plate which was mechanically clamped to the bottom surface of a beam. When so clamped the plate

acted as a cantilever beam. Initially the free end was given deflection of about 1 1/2 in. and anchored by a fine wire cable to a fixed reference on the ground. Deflections of the member in relation to the fixed reference were registered as a change in strain in the plate from that induced by the initial fixed deflection. The gages had been calibrated at the Bureau of Public Roads Research Laboratory prior to installation. The deflection gages were clamped to the beams at a section 14 in. south of the section on which the strain gages were located. Two deflection gages were placed on each of beams 1 and 2. These gages were located 10 in. on either side of each beam centerline in order to detect any rotational movements in the beam.

Other sections further from midspan were also gaged like the section shown in Fig. 2. Since these sections experienced less than maximum live load deflection and strain, data from these sections were not used in this report.

2.3 SITE PREPARATION

Following arrival on the site of the research team with the instrument van, portable scaffolding was erected to provide access to the points to be gaged on the underside of the bridge. Each strain gage location was carefully selected with regard to soundness of the concrete,

and was prepared for the installation of the gage by light sanding, cleaning with acetone and sealing with diluted SR-4 cement. The strain gages were applied with undiluted SR-4 cement after the initial seal coat had cured. Gages exposed to direct contact by rain were thoroughly waterproofed. Dummy gages to complete a Wheatstone bridge circuit were connected to each active gage, and signal transmitting cables were strung from each gage to the instrument van which had been parked beneath the bridge. Inside the van, the recording instrumentation consisted of 48 channels of Consolidated Electrodynamics Corporation System D feeding three 18-channel light beam recording oscillographs. The recording instruments are shown inside the van in Fig. 3. Strain gages were installed on the upper surface of the bridge deck slab with special provision for withstanding severe mechanical abrasion and prolonged immersion in water. Strips of 1 in. wide red plastic tape were sealed to the bridge deck the full length of the span as guide lines for the test vehicle driver in traversing the prescribed paths. Precise levels were taken at 1-ft. intervals 75 ft. each way from the test section along these paths to provide an indication of the smoothness of the actual bridge longitudinal profile.

Pneumatic hoses installed across the bridge deck at three locations were connected to the recording oscillographs to provide instantaneous event marks on each strain record, indicating the passage of each test vehicle axle. Communication between the test vehicle driver, traffic control men and the instrument van operator was by a combination of short wave radio and voice intercom system. Just prior to the beginning of a test series all gage circuits were checked, balanced and calibrated to insure fidelity and accuracy of the recorded data.

2.4 TEST VEHICLE

The Bureau of Public Roads Bridge Research Test Vehicle used in this study was a three-axle Diesel tractor semi-trailer combination which, when properly loaded with any heavy material, closely simulates an H20-S16-44 design vehicle. A photograph of the test vehicle as used on a previous study is shown in Fig. 4. The actual weights and dimensions of the test vehicle as used for the tests described herein are shown in Fig. 5. This vehicle has been used on a large number of bridge research tests on various types of structures in various states. Strain gages in a number of configurations are mounted on the axle housings of the driver and trailer axles of this vehicle between each of the four spring pad and wheel sets.

These gages have been calibrated at the Bureau of Public Roads Laboratory to relate the bending strain in the axle housings to the varying loads on the individual wheels. As the vehicle moves, the axle housing strains are recorded on light beam recording oscillographs mounted on the test vehicle. An indication of the dynamic reactions of each wheel of the moving vehicle is therefore available. Since these data are presently quite complex to reduce and correlate with bridge responses, only some qualitative analyses and frequency determinations have been incorporated in this report.

2.5 TEST PROCEDURE

The analysis of dynamic tests involves the reduction of data from each gage record for runs made with the loaded test vehicle crossing the bridge at nominal speeds from 10 mph to 42 mph on various prescribed paths. The paths on which the driver centered the vehicle are shown in Fig. 2. Deviations of the vehicle from the prescribed path on each run were measured at three points on the path as a means of determining vehicle placement accuracy. Table 1 gives a complete history of the dynamic test program. The average speed of the vehicle from one end of the bridge to the other was measured in the field with a precision timer, and was generally very close to the nominal figure as noted in

the table. The five vehicle paths were selected to provide a systematic variation of the loading to each of the four box beams. The speeds were chosen to give a close and equal spacing of nominal test speeds over the range attainable in a reasonable number of runs. From one to three replications of each run were made as deemed appropriate. Direction of approach was another variable studied, but as indicated previously the speed of the approach from the north was limited by the sharp turn in the roadway and the uphill grade, precluding any but 10 mph runs in the south-bound direction. Paths 1 and 5 were run only at 10 mph because concern for the safety of the driver and vehicle precluded attempting to maneuver the extremely heavy load at higher speeds in such close proximity to the curb. This does not imply that a heavy load might not occur on paths 1 or 5 with possible significant effects as discussed later in this report.

A special group of four runs designated "I" for "aggravated impact" involved driving the test vehicle at 15 mph across 2-in. stepped ramps placed on each wheel track at the gaged section. Two of these runs were made along each of paths 2 and 3.

2.6 REDUCTION OF RECORDS

The three recording oscillographs produced simultaneous photographic traces for each gage during each test run. Each trace provided a complete time history of the gage response in the form of variations about an initial static position in proportion to the actual strain or deflection being experienced by the gage during the passage of the live load. Oscillograph records were taken on 200-ft. rolls of photographic paper each of which might contain from 40 to 70 runs with frequent intermediate calibrations of each gage circuit. As each roll of paper was completed it was immediately put through a processor, and then rapidly scanned to insure that all data had been properly recorded.

Following completion of the field tests, the analog records were reduced to numerical values of strain and deflection. This was done by a combined graphical and mathematical procedure in which the trace deviation from the static position is scaled, compared to a trace deviation for a previous calibration and then reduced to strain or deflection in a formula involving particular gage constants, the appropriate signal attenuation and the length of the interconnecting cable. For dynamic analysis the values taken from the records include the peak and mean responses and the frequency of vibration

of the bridge for each run while the bridge was fully loaded with the test vehicle. After the vehicle had passed, the fundamental natural frequency of the bridge was determined. In addition the logarithmic decrement of vibration was obtained on certain runs by scaling the decreasing amplitudes of successive decaying cycles of vibration and applying the formula

$$\text{Logarithmic decrement} = \frac{1}{n} \ln \frac{A_0}{A_n}$$

Where n = the number of cycles of vibration

$\frac{A_0}{A_n}$ = the amplitude ratio of the first to the n th cycle

The logarithmic decrement provides a common mode of expression of damping characteristics in many field bridge test reports.

3. TEST RESULTS

The dynamic response of a highway bridge under moving load is dictated by the coupled effects of the multi-degree of freedom vibration of the vehicle, the approach and deck profile smoothness and the vibration characteristics of the bridge elements. In this dynamic response study, each of these factors has been accurately recorded by means of the described test procedures.

3.1 DECK PROFILE SMOOTHNESS

Level readings taken along the five prescribed vehicle centerline paths on the bridge were reduced to relative grade elevations. Tables 2A and 2B demonstrate the degree to which the bridge deck profile along each of the five vehicle paths varied from a smooth profile. For analyzing dynamic response the variation from a smooth profile is more relevant than deviation from design grade. The maximum deviations from smooth grade were of the order of 0.052 ft. over a 15-ft. distance (Table 2A) or 0.044 ft. over a 5-ft. distance (Table 2B). Variations are slight both laterally and longitudinally in the south half of the bridge, the direction from which the test vehicle was required to approach the bridge for all speeds over 10 mph. The greater roughness in the north 75-ft. segment is due to the joint at the end of the shorter approach span at that end of the bridge.

3.2 BRIDGE RESPONSE

The three characteristics of dynamic behavior of a bridge structure previously mentioned, strain and deflection dynamic amplifications, fundamental natural frequency of vibration and damping characteristics, have each been investigated in relation to vehicle speeds, paths and directions.

Tables 3A, 3B, and 3C list the crawl, mean and peak deflections, respectively, measured by the deflection gages near midspan on each beam. Crawl run values listed are the minima of the three northbound runs made in each path since it was logically assumed that some slight dynamic response might be present in crawl runs, and that the least values observed would be more nearly representative of the static live load effect. The values recorded are the maxima occurring in any gage on any run corresponding to the greatest magnitude of an influence line. Conversely, peak values listed are the maxima of three replicate runs. The slanted lines between deflection readings indicate the direction of rotation as indicated by the paired gages on beams 1 and 2. This procedure is also followed for strain analysis. Fig. 6A and Fig. 6B show characteristic deflection gage responses at various speeds which aid in understanding the manner in which the magnitudes vary with speed, supplementing the numerical

values in the tables. Heavy lines in the tables enclose those values with which this study is concerned since the primary interest of this investigation is peak dynamic responses which are superimposed on the maximum static live load effects in any member. This procedure is followed in other tables as well, and these values will be designated hereafter as the significant strains, deflections and amplifications.

The base and peak strains recorded on the bottom surfaces of the beams are tabulated in Tables 4A and 4B respectively. In addition to the crawl run strains, mean strain values for northbound 10 mph runs are also shown in Table 4A to demonstrate the validity of the crawl run values as a basis for computing amplifications. This verification was introduced because of the occurrence of negative amplifications. The close similarity of crawl and mean values emphasizes the validity of the crawl run values as a basis for computing amplifications.

Many of the peak strain values for 10 mph and 34 mph runs are lower than the minimum crawl run values (Table 4B). Deflection values are also low at these speeds. This phenomenon is discussed in detail later in this report.

Deck gage strains comprise the third major element of interest. Deck slab strains were less consistent than beam strains, and therefore, no amplifications were calculated.

The most logical crawl values have been selected and shown with peak values for deck strains in Table 5. Diaphragm crawl strains were much more consistent, and crawl and peak values of the diaphragm strains are shown in Table 6.

Longitudinal strain gages on the deck slab were observed to register compressive strains for all runs, indicating a neutral axis located somewhere below the slab. A detailed study of neutral axis location is presented in the companion report previously mentioned. Since transverse deck gages exhibited strain reversals for different vehicle paths, these gages were of prime interest in a dynamic analysis. It should be emphasized that the deck slab strains described are not principal strains at the gage location, but are used only to measure the dynamic response of the deck slab.

Logarithmic decrements of vibration for describing the damping characteristics of the bridge were obtained from deflection data on two impact test runs. To gather the needed data, the oscillograph recorders were left running after the vehicle had completed its passage. A typical decay curve is seen in Fig. 7, together with logarithmic decrement values obtained from this and other similar traces.

The fundamental natural frequency of the unloaded structure was always 6.4 cps, regardless of the frequency

noted while the structure was loaded by the test vehicle. The loaded frequencies varied considerably and are tabulated in Table 7.

4. DISCUSSION OF RESULTS

4.1 BEAM RESPONSES

The test results were examined for the variation of dynamic amplifications for the most highly deflected beam for each run considered. The amplification is expressed as a percentage of the least crawl deflection value for the same test path and direction. Unfortunately the tests in path 1 had to be limited to 10 mph. The significant deflection amplifications on these runs were much higher than significant deflection amplifications for 10 mph runs in other paths suggesting that proportionately higher values might have been experienced at higher speeds. Deflection amplifications are given in Table 8. Mean deflections and peak deflections were correlated for one path to determine the peak semi-amplitudes of vibration as a function of speed. These values are shown in Table 9. Both the peak absolute amplification (Table 8) and the semi-amplitudes indicate that peak dynamic responses for smoothly rolling loads were obtained at 18 mph in path 3. Table 8 further shows that the peak responses for paths 2 and 4 were at 26 mph and 18 mph respectively. While the lowest peak dynamic responses occurred at 34 mph, the semi-amplitudes were not lowest at this speed. It will be remembered, however, that the mean values of deflection

at 34 mph (Table 3C) were nearly as low as the crawl values which explains the apparent anomaly.

The bottom surface strain amplifications were analyzed for evidence of correlation with speed. Table 10 lists the strain amplifications for the most highly strained beam for each run considered, using crawl runs as the base. Negative amplifications seen at 10 mph and 34 mph are not unique, having been observed by others on several types of bridges.⁶ While no recognition has been given to this phenomenon as a positive aid in moving heavy overloads across existing bridges,⁷ the opportunity for exploiting this concept offers promise.

In Table 10 the significant amplification percentages developed under the aggravated impact tests (95.2% maximum) are much higher than have been found in comparable tests on steel I-beam bridges of similar span lengths^{3,4} and generally confirm the observations of A. Rosli⁵ made on European prestressed concrete bridges of various types which indicate that such bridges are quite sensitive to this type of shock loading.

At this point it may be well to emphasize that the occurrence of such low speed shocks is not an entirely remote possibility. These shocks could be caused by a heavily loaded vehicle passing over miscellaneous features, causing a blow similar to that created by the

ramp. Such impact raisers might be frozen, rutted slush, compressed clay balls tracked on the roadway by farm or construction equipment or miscellaneous obstructions such as small pieces of lumber or tools that may occasionally fall from passing vehicles. A final aspect of the aggravated impact effect is the distinct correlation with speed which is plotted in Fig. 8.

For the smoothly rolling loads, peak amplification percentages are as high as 39% for deflections and 25% for strains. No consistent correlation between strain and deflection amplifications has been noted on other single span bridges studied^{3,4}, and no conclusions are drawn here in this regard, except to note that strain amplifications are consistently lower than deflection amplifications. Somewhat contrary to the case for deflection amplifications, the significant strain amplifications reach peak values at 18 mph for all paths. As was the case for deflections, the minimum strain amplifications occur at 34 mph. It must be remembered that there is no way of knowing that the peak amplifications should occur at 18 mph or 26 mph, since it is conceivable that all strains and deflections might reach maximum values simultaneously at some intermediate speed.

The nearly identical semi-amplitudes of vibration of

each beam associated with low average amplitudes at certain speeds (Table 9) suggests that the bridge vibrates with uniform dynamic displacement at these speeds. This phenomenon was noted on other bridge studies⁵. At other speeds, however, less uniformity is evident, suggesting the possibility that transverse vibrations are occurring at some higher mode at these speeds. Such higher modes have been observed when they were purposely induced in highway bridges through use of a mechanical oscillator, in order to study the higher frequencies attainable⁸.

The occurrence of maxima and minima in the dynamic amplifications at 18, 26 and 34 mph could not be ascribed to any forcing frequency of axle passage. All of the strain and deflection trace patterns were studied to determine possible causes of the variations in amplifications. Replicate runs were found to be distinctly similar, eliminating any explanation based on random behavior, and also discounting the theory that the initial position of the sprung load of the vehicle as it comes on the bridge is a major factor. Since the initial sprung load position should be random in itself, there should be a random variation in the bridge response on replicate runs if the sprung load is significant.

The paired deflection gages on beams 1 and 2 generally behaved in the manner expected. As indicated by the slanted lines in Tables 3A and 3B the inner edge of beam 1 consistently deflects more than the outer edge, indicating the tendency of the structure as a whole to deflect transversely in a concave pattern. Beam 2 behaved similarly except when the vehicle was over or outside the beam. The paired strain gages on beam 1 exhibited the opposite effect from the deflection gages, and those on beam 2 exhibited a random effect. Since the beam bearings are parallel to the roadway crown and the bridge is "dishing" under the test vehicle load, a slight twist is imparted to the beams when the bridge is loaded. An examination of the strain gage response in each beam as the vehicle traverses the bridge in each of the five paths successively shows a consistent symmetry of response. Thus, the validity of the unexpected strain relationship between the paired gages may be accepted as the true response in the beam and not a gage discrepancy.

Two significant aspects of the dynamic behavior stand out as a result of the analysis and comparison of individual run records: (1) the vibrations while the vehicle is on the bridge may follow either a nearly pure harmonic pattern, a ragged irregular pattern or a beating pattern,

and (2), the loaded frequencies range from 2.5 cps to 9.0 cps at the various speeds. The variations in both instances appeared to relate to speed, but the presence or absence of a harmonic vibration was not related to the magnitude of amplification. Of most significance was the fact that the loaded frequency at 18 mph, the critical speed for amplification was the natural fundamental frequency of the bridge. The loaded frequency at 34 mph, the speed at which amplifications were least, was 8.7 cps which was nearly the highest frequency noted. Although a mathematical expression for this effect was not sought, the evidence clearly shows that the coupling of the vehicle and bridge vibrations at one or more critical speeds develops a transient of peak magnitude when the resulting loaded frequency is the same as the bridge natural frequency.

4.2 DECK SLAB RESPONSES

The analysis of the deck slab strains revealed that the live load strain at any point varies in accordance with a strain pattern which may be separated into three distinct components, each of which may be absent or present according to the vehicle placement and speed.

These components are;

1. A smoothly varying strain resembling a live load response under a vehicle with infinite lateral width. This

strain may be tensile or compressive.

2. A more or less acute peak strain superimposed on the above, and caused by the contact pressures under the individual wheels. This can be thought of as a small travelling shock wave. This strain is always tensile even if the smoothly rolling effect is compressive in which case the latter may suddenly be reversed for a brief instant.

3. The harmonic transient vibration induced by the vehicle motion superimposed on both of the components above.

This characteristic response pattern was also noted in the strains on the bottom surface of the beams, except that the effect described in item 2 was greatly attenuated through the depth of the beam, as might be expected.

This characteristic strain pattern has not been analyzed in detail. The peak values described in item 2 above have been included as a valid part of the maximum strain excursions whenever they were present.

Since the deck was designed as a series of lateral beam segments with partial end-fixity between the longitudinal beams, the analysis of the dynamic behavior of the deck slab through the responses of the transverse strain gages corresponds to the design approach. These strains are not the principal strains as noted earlier

but provide a useful measure of the dynamic response. The companion report which has been mentioned will investigate the principal strains for static live loading. The longitudinal gages on both top and bottom of the deck slab always registered compressive strains, and therefore, would generally reflect the same dynamic response as the beam bottom surface strains which have been analyzed.

It was noted that the deck behaved as a continuous slab over flexible supports. From the data in Table 5 and assuming direct symmetrical superposition to simulate the effect of two identical test vehicles on the bridge, a qualitative pattern of the transverse flexural deck action has been synthesized in Fig. 9. As can be seen from the relative peak strains indicated, a sudden live load strain reversal of substantial magnitude can be induced transversely in the deck slab adjacent to the inner edge of a beam by vehicles crossing the bridge on different paths consecutively. For example, the test vehicle crossing the bridge on path 2 at 42 mph induces a peak strain of +51.2 microinches-per-inch on the underside of the deck near the inner edge of beam 2. A similar vehicle following on path 4 at 26 mph would induce a strain of -30.4 microinches-per-inch at the same point. Confirming that the indicated flexure in the slab is not a

localized surface effect is the relative response of two parallel transverse strain gages on the deck slab one above the other on top and bottom of slab near the inner edge of beam 1 as shown in Table 11. The extreme ranges of strain reversal are very nearly identical for both top and bottom gages. For these two gages the strains were opposite in sign for all loadings indicating transverse flexure about a neutral axis within the deck slab. Since the noted live load strain reversals may influence the fatigue of the deck slab and may therefore play a significant part in some deck slab failures, the recognition of this possibility should give rise to further investigation of this finding by designers and other researchers.

Analysis indicates that the critical speeds for deck slab strain amplifications differ from those noted for the maximum beam responses. Also the aggravated impact runs had only the same effect on significant strains on the slab surface as did the smoothly rolling runs. With regard to live load strain reversals, the maximum and minimum values always occurred at different speeds. Dynamic effects at the deck gage point near the inner edge of beam 1 when the static live load effect was also a maximum were only available for 10 mph runs. The deck gage near the outer edge of beam 2 experienced no strain

reversal. The deck gage near the inner edge of beam 2 experienced strain reversal and an amplification of 82% in the direction of tension. The latter observation suggests that much additional valuable information on bridge deck slab live load behavior leading to an improved deck design might be obtained from a more comprehensive study of deck strains.

The dynamic strains at the top of the parapet have been tabulated in Table 12, and show that the path 1 runs for which only 10 mph speeds were used cause the greatest live load response, and that all strains are compressive. A correlation of these strains with those produced in the bottom surface of the beams was sought to determine the possibility of extending these field bridge studies on the basis of parapet gages which could be installed on many bridges easily and quickly. While some correlation may be possible, the evidence in this study precludes reliance on such a procedure.

4.3 DIAPHRAGM RESPONSES

The strain gages on the bottom surfaces of the transverse midspan diaphragms were intended to provide a determination of the degree of participation of these elements of the bridge in distributing the live load to the beams. The observed strains indicate that the diaphragms behave as deep fixed-end beams which develop points of inflection

for some loadings. The smoothly rolling loads produced maximum strains greater than any observed in beam or deck gages. Some maxima occurred at 34 mph when the beam amplifications were least. The strains found in the gages on the bottom surfaces of the diaphragms are shown in Table 6. The importance of the diaphragm as a load distributing element will be the subject of another study. If it is found that these members comprise a necessary element of the structure, the strain reversal and amplification noted in this study will provide useful design guides for any proposed modification.

4.4 TEST VEHICLE RESPONSE

Fig. 10 shows typical segments of records of the response of one of the test vehicle trailer axle housing gages. The vertical oscillations represent the combined tire and leaf spring vibration effects. Since only a phenomenological analysis of the response is to be made in this instance, no magnitudes have been computed for the oscillations. The frequencies observed are 2.5 cps for the 10 mph runs and 3.3 cps for the higher speeds. There is little apparent difference in the 18 mph and the 34 mph responses although the bridge responses were at opposite extremes at these speeds. At 34 mph and at 42 mph, the typical vehicle response displays an almost completely damped vibration while the trailer axle is on the bridge, and a sudden reappearance of significant vib-

ration amplitudes as the vehicle begins to leave the structure. The lack of an obvious correlation of bridge and vehicle vibrations is contrary to the usual assumption made in analytical studies that such a correlation exists. The test vehicle studies that preceded this research established 2.9 cps as the natural frequency of vibration on the tires and 7.7 cps as the natural frequency of the sprung load. Neither of these frequencies is evident in the test vehicle records although the 10 mph runs show a frequency close to that of the vibration on the tires.

4.5 DIRECTIONAL EFFECT

Significant strain and deflection amplifications are distinctly greater for the southbound runs on paths 1 and 4 as seen in Table 13. On path 2 the northbound run amplifications are greater and on path 3 the evidence is inconclusive. Based on the profile data, it was anticipated that all southbound runs would show greater amplifications. That they do not may be attributable to the fact that the profiles were not taken exactly on the wheel tracks, and that 10 mph may not be sufficient to bring out roughness effects for a heavily loaded vehicle.

4.6 DAMPING EFFECT

As shown in Fig. 7, logarithmic decrements of vibration amplitude are not uniform at different points for

identical cycles of vibration, although the variation is slight. This is consistent with similar observations reported by others⁴. The damping characteristics of this bridge lie somewhere between those noted for flexible and for stiff composite steel beam spans of about the same length described in the cited report. The logarithmic decrements reported herein more nearly coincide with those reported for sway vibrations of tall concrete piers supporting the spans in the cited report.

5. S U M M A R Y A N D C O N C L U S I O N S

The objective of this research is to provide analyses and interpretations of experimental field data obtained through studies of heavy moving load effects on a single span prestressed concrete spread box beam highway bridge. A critical examination of the test results is made in order to determine which of the factors generally held to be of significance in trial attempts to find analytical solutions of the dynamic behavior of highway bridges are, in fact, of importance, and which may be disregarded.

A series of test runs along various critical paths has been conducted with a test vehicle approximating an H20-S16-44 design load, while continuous strain and deflection readings were being taken at critical points on the bridge. The dynamic amplifications of static live load strains and deflections have been correlated with test vehicle speed and placement and with deck profile smoothness in order to establish critical parameters for future analytical studies.

The strains and deflections measured in this study were quite small, reflecting the strength and the stiffness of the structure which are being investigated in detail and compared with design values in a companion report by others.

The overall consistency of the data, as evidenced by the similarity of replicate runs and the symmetrical pattern of strain and deflection variation as the vehicle traversed the bridge on various paths, lends credence to the validity of the field measurements supporting the findings.

It was found that the strains at the bottom surface of the beams experienced a greater amplification under impact loading than did those recorded in the tests of other bridge types of comparable span lengths. While deflection amplifications under impact loading were not available, the fact that deflection amplifications are consistently higher than strain amplifications for smoothly rolling loading suggests that deflection amplification under impact loading was exceedingly high.

Maximum and minimum dynamic strain amplification at the bottom surface of the beams occurred at test vehicle nominal speeds of 18 mph and 34 mph, respectively. A detailed study of the individual runs revealed that a very slight variation from the nominal speeds resulted in striking changes in the vibration response pattern of the various gages. From this behavior, it may be concluded that an infinite number of critical speeds would have to be determined if bridge design were concerned with the dynamic effect of all conceivable load-axle spacing combinations.

An analytical comparison of the test vehicle and bridge records taken simultaneously divulged no apparent correlation of the two dynamic responses, either through

consideration of the variation in the vehicle initial sprung load position or of the frequency of axle passage. The resulting loaded frequency, at certain critical speeds for the particular bridge-vehicle combination involved in this study, is a factor which can be correlated with maximum amplifications. (A loaded frequency of vibration which is the same as the natural unloaded frequency causes maximum amplifications.) Conversely, a high loaded frequency is conducive to low amplifications.

Transverse dynamic live load strain reversals were found in the deck slab near the inner edge of the beam. While the live load reversal does not signify a reversal of the total live and dead load strain, it does show that the dynamic strain range is great enough to make fatigue failures of the deck slab a matter of concern.

The maximum live load strains on any element of the structure were measured on the bottom surfaces of the diaphragms, which behaved as deep fixed-end beams. While the true value of the diaphragm as a load distributing element will have to be resolved following completion of an impending study directed at this question, the findings of this study indicate the rather substantial participation of the diaphragm in the dynamic action.

The effect of the smoothness of the bridge deck profile on the dynamic amplifications was not conclusive, due mainly to the fact that the runs investigating this variable had to be limited to 10 mph.

6. N O M E N C L A T U R E

AASHO	American Association of State Highway Officials
cps	cycles per second
crawl	the minimum steady forward speed of the test vehicle - about 2.5 miles per hour
H20-S16-44	a theoretical three-axle design vehicle with an eight-kip front axle 14 ft. ahead of a 32-kip drive axle and followed by a 32-kip trailer axle 14 ft. to 30 ft. behind the drive axle
ln	the logarithm to the base e
mph	miles-per-hour
run	one passage of the weighed and measured test vehicle across the bridge on a designated path at a constant predetermined speed
semi-amplitude	the difference between the mean and the peak deflection of a beam vibrating under a passing load
SR-4	a trademark designation of strain gages and strain gage cements manufactured by BIE Electronics, Waltham, Massachusetts
System D	a strain gage signal conditioning and amplifying system manufactured by Consolidated Electrodynamics Corporation, Pasadena, California

7. T A B L E S

Table 1 Test Run Replication and Variation

Vehicle Nominal (mph)	Speed Actual Range (mph)	Vehicle Path					Average Maximum Lateral Deviation (inches)
		1	2	3	4	5	

Smoothly Rolling Runs

10	9.7-10.1	2	2	2	2	2	1.7
10(S)	9.7-11.2	1	2	2	2	-	1.3
18	18.3-20.6	-	2	2	2	-	2.0
26	25.9-27.9	-	2	2	2	-	1.3
34	33.9-35.2	-	3	3	3	-	1.6
42	40.8-41.7	-	3	3	3	-	1.0

Impact Runs

15(S)	11.9-13.8	-	2	2	-	-	2.5
-------	-----------	---	---	---	---	---	-----

(S) - Southbound Runs. All other runs northbound

Table 2A Profile Grade Increments

(ft. x 10⁻²)

Distance from Gaged Section of 15' Segments Along Vehicle Path	Vehicle Path				
	1	2	3	4	5
60'-75' south	44	43	42	41	41
45'-60' south	41	41	41	41	41
30'-45' south	42	42	41	42	42
15'-30' south	40	41	43	42	42
0'-15' south	43	43	42	42	40
0'-15' north	43	42	42	42	44
15'-30' north	42	42	42	44	43
30'-45' north	39	39	40	39	38
45'-60' north	43	42	38	39	39
60'-75' north	40	39	47	41	44
<u>Average</u>	<u>41.7</u>	<u>41.4</u>	<u>41.8</u>	<u>41.3</u>	<u>41.4</u>

Table 2B Maximum Profile Grade Deviation for all 15' Segments
(Path 1, 45'-60' South of Gaged Section)

Incremental Distance Along Vehicle Path	Profile Grade Increments		(ft. x 10 ⁻³)
	Planned Grade	Actual Grade	Difference
0'	0	0	0
1'	27	20	7
2'	54	40	14
3'	80	50	30
4'	107	70	37
5'	134	90	44
6'	160	120	40
7'	187	160	27
8'	214	190	24
9'	240	220	20
10'	267	250	17
11'	294	280	14
12'	320	310	10
13'	347	340	7
14'	374	380	6
15'	400	400	0

Table 3A Crawl Run Deflections
 (Minima of Three Northbound Runs; in. x 10⁻³)

Vehicle Path	Beam				
	1	2	3	4	
1	80	80	71 — 68	48	26
2	59	— 61	72 — 70	59	33
3	44	— 46	67 — 70	70	45
4	32	— 34	52 — 55	75	60
5	23	— 24	40 — 45	72	82

Table 3B Speed Run Peak Deflections
 (Maxima of All Northbound Runs; in. x 10⁻³)

Vehicle		Beam			
Path	Speed (mph)	1	2	3	4
1	10	104 — 105	94 — 85	56	30
2	10	74 — 77	92 — 90	68	39
2	18	77 — 79	94 — 94	74	44
2	26	84 — 86	100 — 94	73	45
2	34	75 — 81	84 — 90	70	41
2	42	75 — 81	85 — 87	68	39
3	10	51 — 55	81 — 82	84	54
3	18	59 — 61	90 — 94	95	60
3	26	56 — 60	84 — 84	88	56
3	34	53 — 55	70 — 79	81	53
3	42	57 — 62	79 — 86	88	58
4	10	35 — 39	65 — 68	88	70
4	18	44 — 47	72 — 83	102	81
4	26	39 — 43	70 — 78	98	77
4	34	43 — 45	61 — 71	90	74
4	42	47 — 50	67 — 73	98	79
5	10	28 — 30	51 — 55	90	102

Table 3C Speed Run Mean Deflections
 (Maxima of All Northbound Runs; in. $\times 10^{-3}$)

Vehicle		Beam			
Path	Speed (mph)	1	2	3	4
1	10	93 — 92	82 — 77	50	24
2	10	68 — 72	86 — 84	63	34
2	18	71 — 73	87 — 86	67	37
2	26	68 — 68	85 — 79	63	34
2	34	65 — 68	75 — 78	59	37
2	42	65 — 67	75 — 73	56	30
3	10	47 — 51	77 — 78	78	50
3	18	49 — 53	77 — 79	79	49
3	26	51 — 51	79 — 78	82	52
3	34	46 — 49	63 — 71	73	46
3	42	45 — 50	71 — 77	77	52
4	10	33 — 36	61 — 63	85	66
4	18	34 — 37	65 — 70	86	71
4	26	31 — 35	60 — 66	84	64
4	34	36 — 37	54 — 63	80	64
4	42	32 — 36	56 — 61	83	65
5	10	23 — 35	43 — 38	80	91

Table 4A Surface Strains - Bottom Surface of Beam
 (Minima of Three Northbound Crawl Runs
 and Mean Values of Selected Speed Runs; μ in./in.)

Vehicle Path	Beam			
	1	2	3	4
1 Crawl	37.2 / 42.1	34.2 / 29.4	17.4	11.9
Mean	39.1 / 40.5	32.1 / 30.4	18.5	13.4
2 Crawl	30.4 / 29.7	33.5 / 32.8	22.4	17.4
Mean	32.2 / 28.9	34.7 / 34.5	23.6	16.4
3 Crawl	25.0 / 20.4	28.7 / 33.3	29.4	21.7
Mean	23.0 / 20.9	26.5 / 29.3	27.4	23.8
4 Crawl	18.8 / 17.2	23.4 / 24.4	33.6	29.6
Mean	19.3 / 12.9	23.5 / 22.4	32.8	29.7
5 Crawl	12.4 / 7.1	17.9 / 14.2	30.2	41.2
Mean	13.3 / 9.8	16.8 / 13.8	31.7	46.0

All Strains Tensile

Table 4B Surface Strains- Bottom Surface of Beam
 (Maxima of all Northbound Runs; μ in./in.)

Vehicle		Beam			
Path	Speed (mph)	1	2	3	4
1	10	45.0 / 43.6	34.3 / 33.8	21.2	14.1
2	10	34.0 / 31.2	37.3 / 38.0	25.8	15.6
2	18	34.6 / 34.7	38.5 / 41.0	25.0	19.8
2	26	38.1 / 35.1	35.4 / 36.3	25.0	20.9
2	34	35.4 / 34.0	35.0 / 34.8	24.3	17.8
2	42	35.0 / 34.7	38.1 / 38.7	25.0	16.4
2	15 I*	59.4 / 51.6	55.0 / 56.0	44.8	40.8
3	10	23.9 / 22.3	28.0 / 33.8	30.8	23.8
3	18	31.4 / 25.8	34.4 / 33.5	34.3	27.8
3	26	28.5 / 26.2	30.5 / 34.5	30.8	26.2
3	34	24.8 / 22.3	28.3 / 32.4	25.8	24.5
3	42	27.1 / 23.2	32.8 / 34.9	31.2	26.8
3	15 I*	55.1 / 46.9	56.0 / 52.9	56.4	48.9
4	10	19.3 / 14.9	25.4 / 24.5	35.8	29.8
4	18	23.0 / 18.7	28.4 / 29.6	39.7	35.6
4	26	22.5 / 17.8	27.2 / 24.8	35.4	35.6
4	34	21.2 / 17.0	26.1 / 23.8	32.4	28.2
4	42	22.1 / 18.7	26.9 / 26.2	38.9	37.4
5	10	15.2 / 11.1	20.5 / 17.3	34.4	50.0

All Strains Tensile

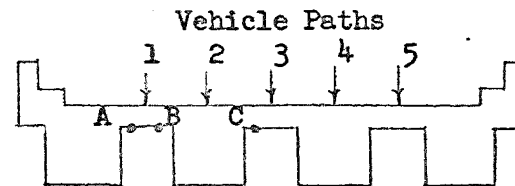
I* - 15 mph Impact Runs

Table 5 Deck Slab Strains

Compressive Strains Shown as Negative (min./in.)

Vehicle		A	Gage B	C	Vehicle		A	Gage B	C	Vehicle		A	Gage B	C
Path	Speed (mph)				Path	Speed (mph)				Path	Speed (mph)			
1	Crawl	18.0	8.3	21.1	3	Crawl	-9.3	8.6	16.1	4	Crawl	-7.3	5.6	-26.8
1	10	16.4	11.2	22.5	3	10	-9.2	12.6	32.9	4	10	-8.8	6.0	-31.2
					3	18	-9.6	5.0	38.0	4	18	-10.0	9.3	-28.8
2	Crawl	15.6	19.5	28.1	3	26	-7.6	16.2	26.0	4	26	-10.4	7.6	-30.4
2	10	-13.2	13.2	50.5	3	34	-8.0	11.2	29.8	4	34	-8.8	9.6	-24.2
2	18	-15.2	33.5	48.5	3	42	-10.0	11.2	29.1	4	42	-10.0	7.6	-29.5
2	26	-18.0	33.0	26.0	3	15I*	-16.8	27.3	36.3					
2	34	-12.8	29.1	49.1						5	Crawl	-6.9	5.3	-16.4
2	42	-14.0	31.4	51.2						5	10	-8.0	4.6	-19.0
2	15I*	-8.4	42.0	51.4										

* 15 mph Impact Runs



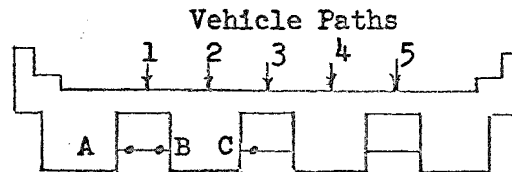
Gage Bottom Surface Transverse Gage Locations

Table 6 Diaphragm Strains

Compressive Strains Shown as Negative (µin./in.)

Vehicle		A	Gage B	C	Vehicle		A	Gage B	C	Vehicle		A	Gage B	C
Path	Speed (mph)				Path	Speed (mph)				Path	Speed (mph)			
1	Crawl	25.7	28.5	10.3	3	Crawl	-7.1	15.6	19.9	4	Crawl	-15.51	-0.4	11.4
1	10	36.2	38.8	12.1	3	10	-4.2	24.8	24.3	4	10	-18.7	0	13.6
					3	18	-7.1	21.3	24.0	4	18	-18.2	0	5.2
2	Crawl	13.6	38.7	18.8	3	26	-6.2	22.1	19.9	4	26	-15.0	0	13.6
2	10	21.0	57.7	19.2	3	34	-4.2	29.4	19.6	4	34	-23.2	0	9.6
2	18	13.8	41.5	24.0	3	42	-5.6	31.0	20.6	4	42	-13.5	0	10.3
2	26	18.7	40.4	21.4	3	15I*	-6.6	34.8	26.0					
2	34	22.1	65.0	18.1						5	Crawl	-19.4	-7.8	1.1
2	42	20.2	63.2	22.8						5	10	-22.5	-11.2	-2.2
2	15I*	29.2	60.4	27.6										

* 15 mph Impact Runs



Diaphragm Bottom Surface Transverse Gage Locations

Table 7 Loaded Beam Vibration Frequencies
(Vehicle at midspan; cps)

Vehicle Speed (mph)	Vehicle Path				
	1	2	3	4	5
10	2.5	N.D.	2.5	2.5	2.5
10(S)	4.0	N.D.	N.D.	2.7	-
18	-	6.4	6.4	6.4	-
26	-	6.4	6.4	5.0	-
34	-	N.D.	8.7	8.0	-
42	-	N.D.	7.2	8.0	-
15I**	-	9.0	6.4*	-	-

(S) - Southbound runs. All others northbound.

* - Transverse gages vibrated at 2.0 cps. with a smaller 15.0 cps. superimposed vibration.

N.D.- No distinct frequency discernible.

** - 15 mph Impact Runs

Table 8 Deflection Amplification
(Percentage Increase over Crawl Run Values)

Vehicle							
Path	Speed (mph)	1	2	3	4	5	6
1	10	30.4	31.2	32.4	25.0	16.7	15.4
2	10	25.4	26.3	27.9	28.6	15.2	18.2
2	18	30.5	29.6	30.6	34.3	25.4	33.4
2	26	42.4	41.2	39.0	34.3	23.7	36.4
2	34	27.1	32.9	16.7	28.6	18.6	24.3
2	42	27.1	32.9	18.1	24.3	15.2	18.2
3	10	15.9	19.6	20.9	17.2	20.0	20.0
3	18	34.0	32.6	34.4	34.4	35.8	33.4
3	26	27.3	30.5	25.5	20.0	25.8	24.5
3	34	20.5	19.6	4.5	12.9	15.8	17.8
3	42	29.6	34.8	17.9	22.9	25.8	29.0
4	10	9.4	14.7	25.0	23.7	17.4	16.7
4	18	37.5	38.2	38.5	51.0	36.1	35.0
4	26	21.8	26.5	34.7	41.7	30.7	28.4
4	34	34.4	32.4	17.3	29.1	20.1	23.3
4	42	46.9	47.0	28.8	32.7	30.7	31.7
5	10	21.7	25.0	27.5	22.3	25.0	24.4

Table 9 Deflection Semi-Amplitudes

From Path 3 Runs of Tables 3B and 3C (in. x 10⁻³)

Vehicle Speed (mph)	Beam				Avg.		
	1	2	3	4			
10	4	4	4	4	6	4	4.3
18	10	8	13	15	16	11	12.2
26	5	9	5	6	6	4	5.8
34	7	6	7	8	8	7	7.2
42	12	12	8	9	11	6	9.7

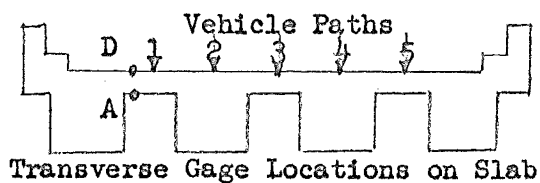
Table 10 Beam Bottom Surface Strain Amplification
(Percentage Increase over Crawl Run Values)

Vehicle		Beam					
Path	Speed (mph)	1		2		3	4
1	10	21.0	3.6	0.3	15.0	21.8	18.5
2	10	11.5	5.1	11.4	15.8	15.2	-10.3
2	18	13.8	16.8	15.0	25.0	11.6	13.8
2	26	25.3	18.2	5.7	10.6	11.6	20.1
2	34	16.5	14.5	4.5	6.0	8.5	2.3
2	42	15.1	16.9	13.8	17.9	11.6	-5.7
2	15 I*	95.5	74.0	64.4	70.6	100.0	192.0
3	10	-4.4	9.3	-2.4	1.5	4.8	9.8
3	18	25.6	26.5	19.8	0.6	23.4	28.1
3	26	14.0	28.5	6.3	3.6	4.8	20.7
3	34	-0.8	9.3	-1.4	-2.7	-12.2	12.9
3	42	8.4	13.7	14.3	4.8	6.2	23.5
3	15 I*	120.4	130.0	95.2	58.9	92.0	125.0
4	10	2.7	-13.3	8.6	0.4	6.6	0.7
4	18	22.3	8.7	21.4	21.4	18.2	20.4
4	26	19.7	3.5	16.3	1.6	5.4	20.4
4	34	12.8	-1.2	11.6	-2.5	-3.6	-4.7
4	42	17.6	8.7	15.0	7.4	15.8	26.4
5	10	22.6	56.4	14.5	21.8	13.9	21.4

I* - 15 mph Impact Runs

Table 11 Comparison of Deck Slab Strains

Compressive Strains Shown Negative ($\mu\text{in./in.}$)



Vehicle Speed (mph)	Gage	Vehicle Path				
		1	2	3	4	5
10	D	-15.5	11.2	11.7	13.6	11.7
	A	16.4	-13.2	-9.2	-8.8	-8.0
18	D	-	13.6	15.6	13.2	-
	A	-	-15.2	-9.6	-10.0	-
26	D	-	15.2	12.0	13.6	-
	A	-	-18.0	-7.6	-10.4	-
34	D	-	11.2	11.7	14.4	-
	A	-	-12.8	-8.0	-8.8	-
42	D	-	9.7	13.6	13.2	-
	A	-	-14.0	-10.0	-10.0	-
15I*	D	-	17.0	22.2	-	-
	A	-	-8.4	-16.8	-	-

*15 mph Impact Runs

Table 12 Parapet Strains

All Runs Northbound (µin./in.)

Vehicle Speed (mph)	Vehicle Path				
	1	2	3	4	5
Crawl	38.3	30.2	22.7	16.0	11.7
10	43.2	33.5	24.3	16.4	12.9
18	-	36.1	28.9	22.2	-
26	-	38.2	26.7	19.3	-
34	-	28.6	19.6	15.0	-
42	-	28.5	20.7	15.0	-
15I*	-	41.2	42.7	-	-

All Strains Compressive

I* - 15 mph Impact Runs

Table 13 Directional Effect
10 mph Peak Strains and Deflections

Path	Dir.	Beam					
		1	2	3	4	5	6
Deflections (in. x 10 ⁻³)							
1	N	104	105	94	85	56	30
1	S	110	111	97	91	60	31
2	N	74	77	92	90	68	39
2	S	73	77	86	87	68	38
3	N	51	55	81	82	84	54
3	S	54	60	80	83	85	54
4	N	35	39	65	68	88	70
4	S	36	40	62	68	91	72
- - - - -							
Strains (µin./in.)							
1	N	45.0	43.6	37.3	38.0	25.8	11.0
1	S	46.5	47.4	39.5	34.5	23.2	13.8
2	N	34.0	31.2	37.3	38.0	25.8	15.6
2	S	35.4	30.0	36.5	36.9	23.5	17.5
3	N	23.9	22.3	28.0	33.8	30.8	23.8
3	S	27.2	22.8	29.8	32.7	29.3	22.6
4	N	19.3	14.9	25.4	24.5	35.8	29.6
4	S	19.3	14.8	25.7	24.2	36.6	33.0

8. FIGURES

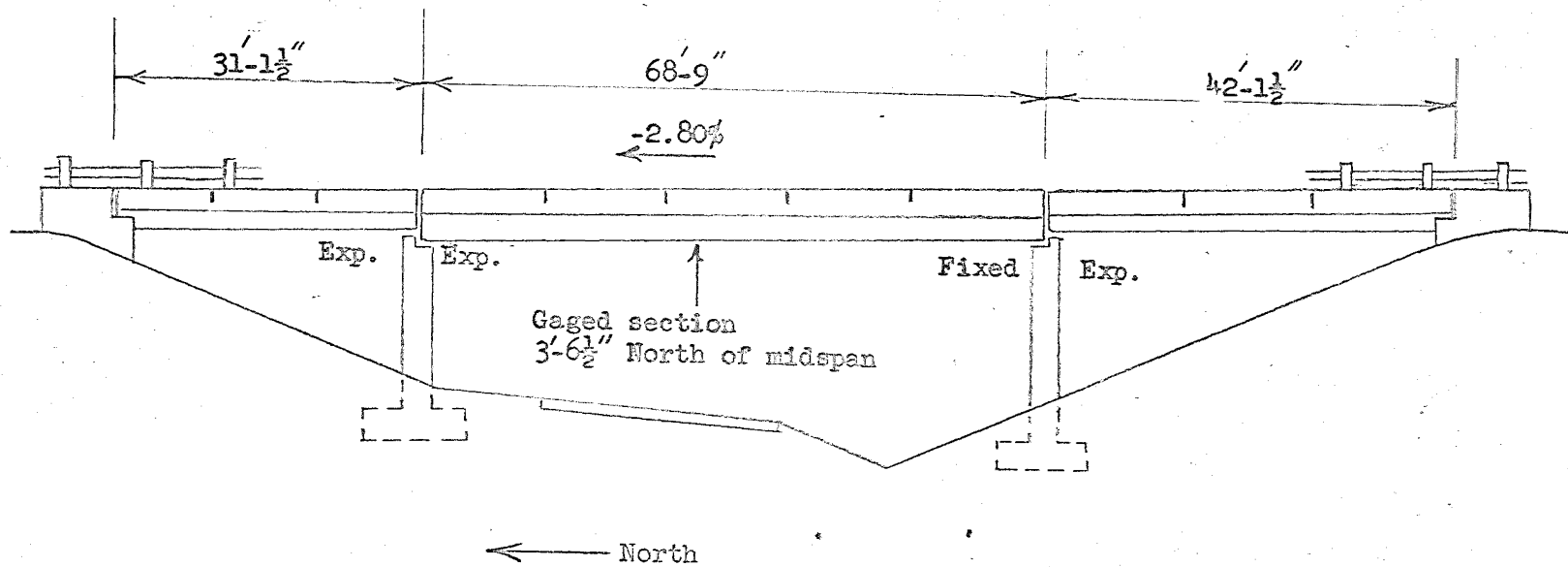
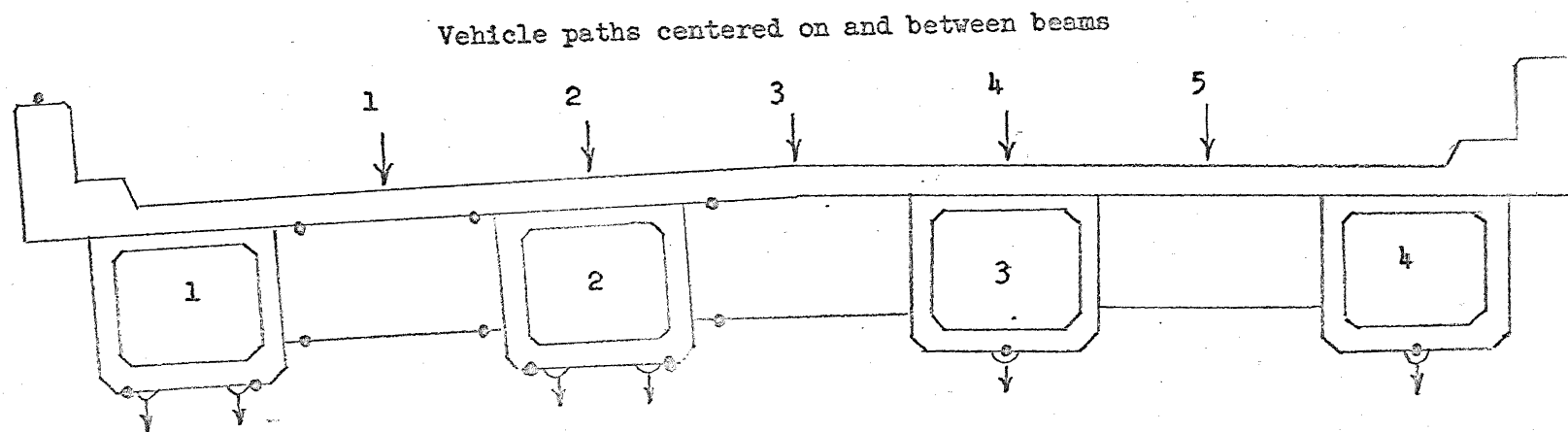


Fig. 1 Test Bridge Elevation Looking East



- Strain gages; longitudinal on beams and parapet; transverse on deck and diaphragm
- ▽ Deflection gages

Fig. 2 Cross-section of Bridge near Gaged Section Facing South

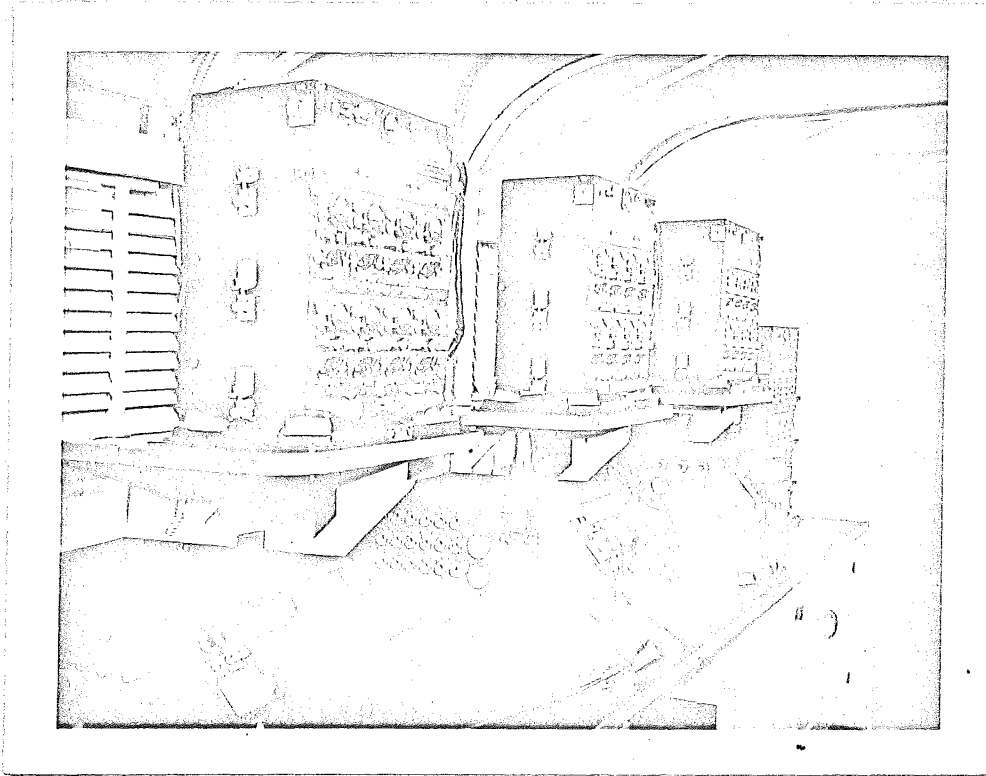


Fig. 3 Interior of Instrument van

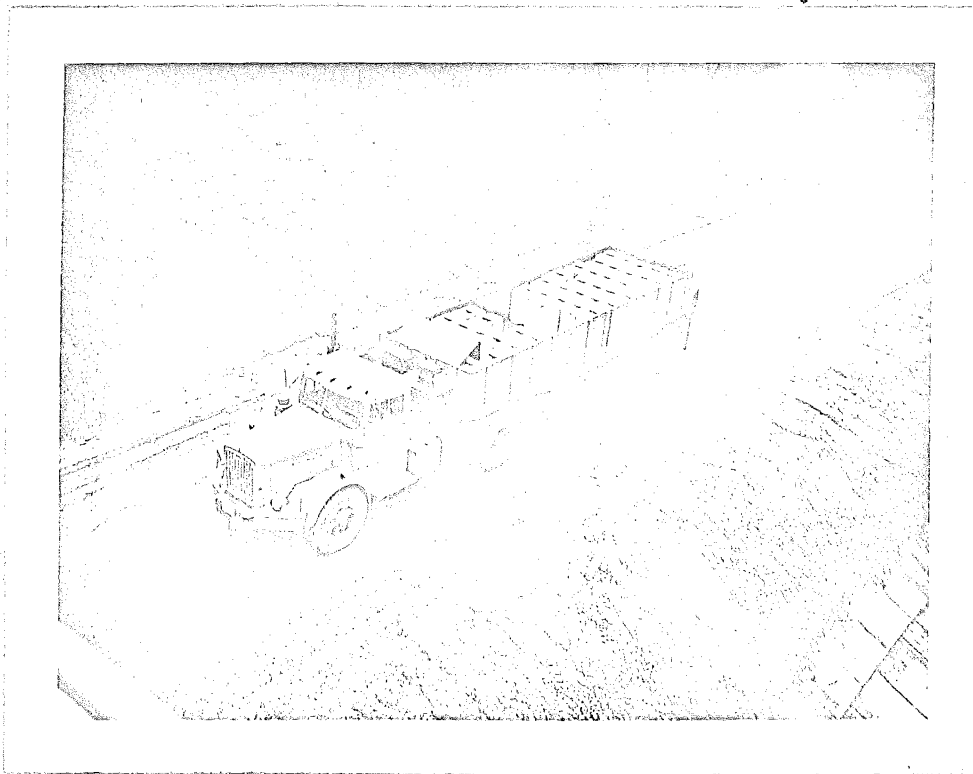
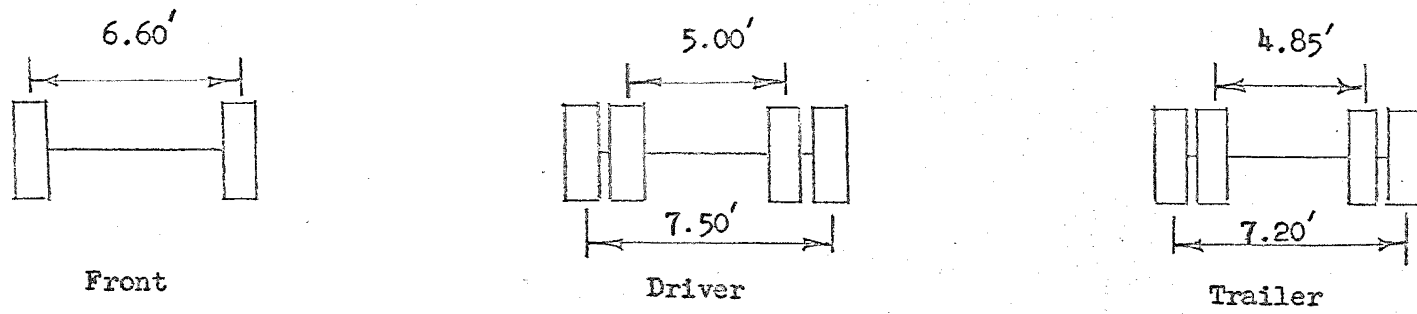
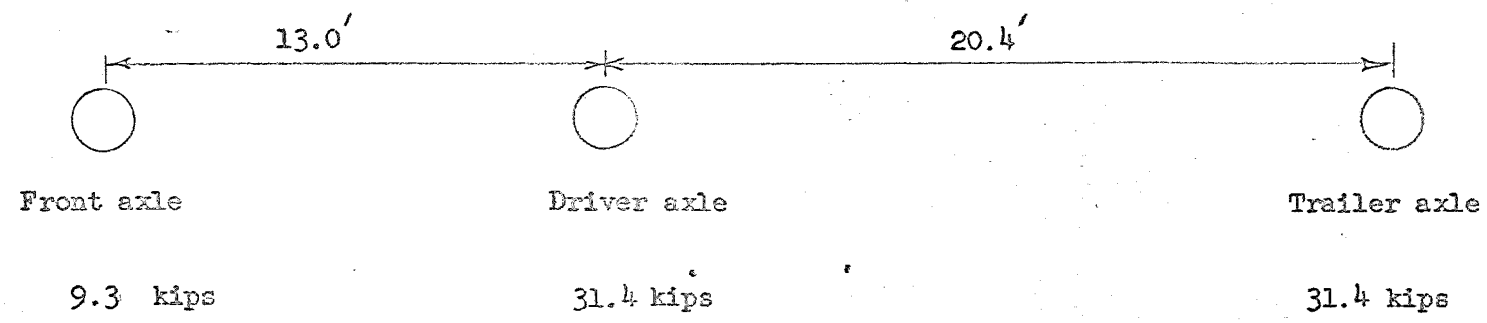


Fig. 4 Bridge Research Test Vehicle

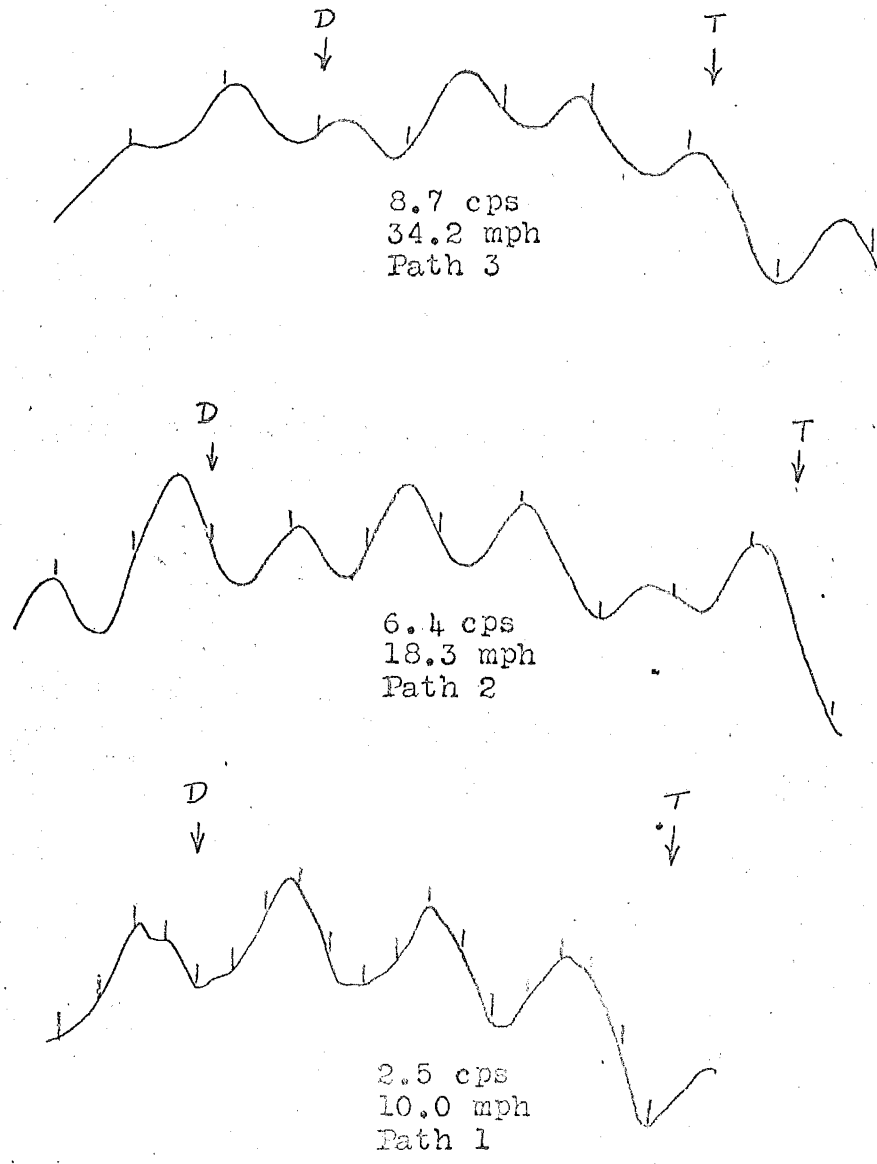


AXLE WHEEL SPACING



AXLE SPACING AND WEIGHT

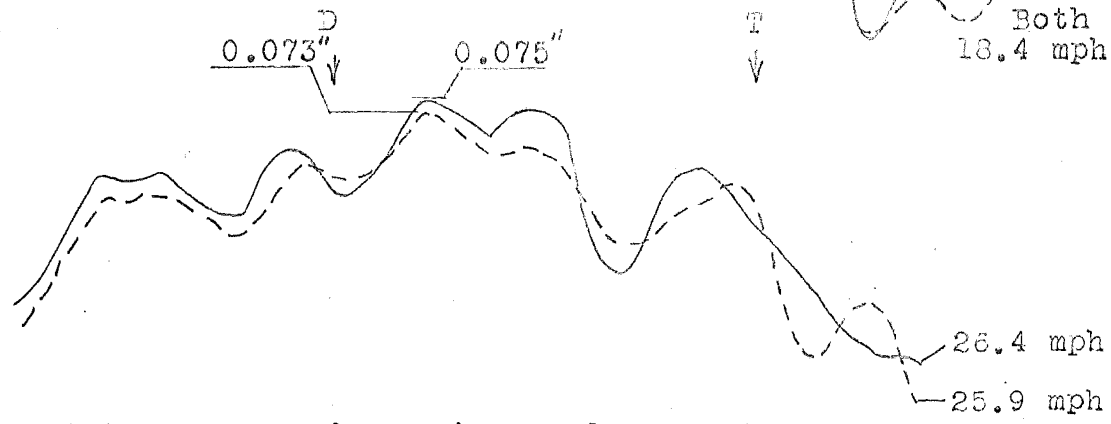
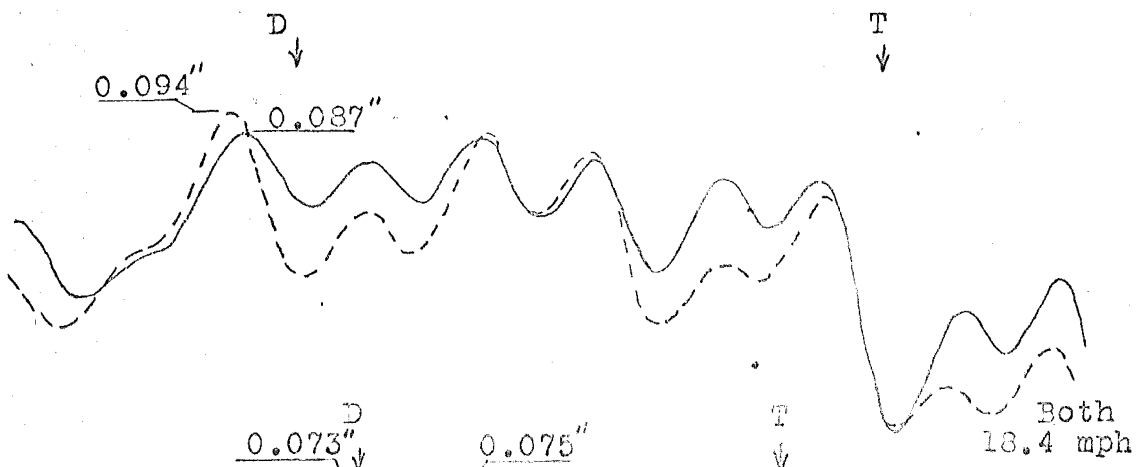
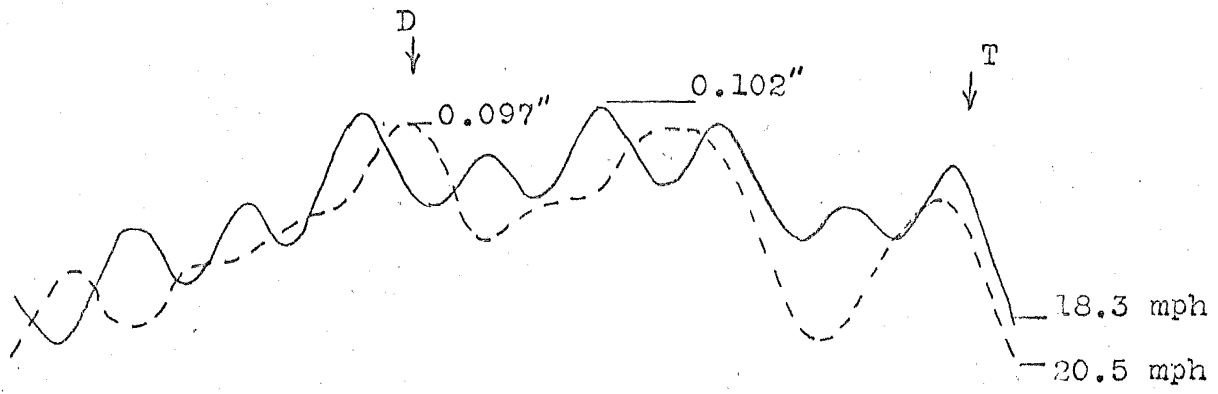
Fig. 5 Test Vehicle Dimensions and Weights



D
↓ = Point on Trace when Driver Axle over Gage

T
↓ = Point on Trace when Trailer Axle over Gage

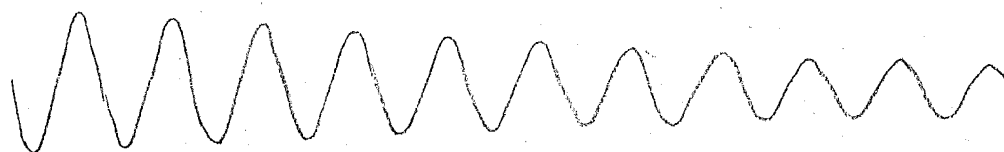
Fig. 6A Bridge Loaded Frequencies
Deflection Gage Records
0.1 Second Time Lines Shown



D
↓ = Point on Trace when Driver Axle over Gage

T
↓ = Point on Trace when Trailer Axle over Gage

Fig. 6B Speed Effect on Bridge Response
Consecutive Runs on Same Path
Same Deflection Gage Traces Compared
Pairs of Traces Normalized to Same Base



Deflection Gage Vibration Decrement Trace

Vehicle Path	Beam					
	1	2	3	4		
2	.094	.096	.101	.089	.097	.107
3	.105	.094	.102	.092	.097	.112

Logarithmic Decrement Values

Fig. 7 Typical Logarithmic Decrement of Vibration

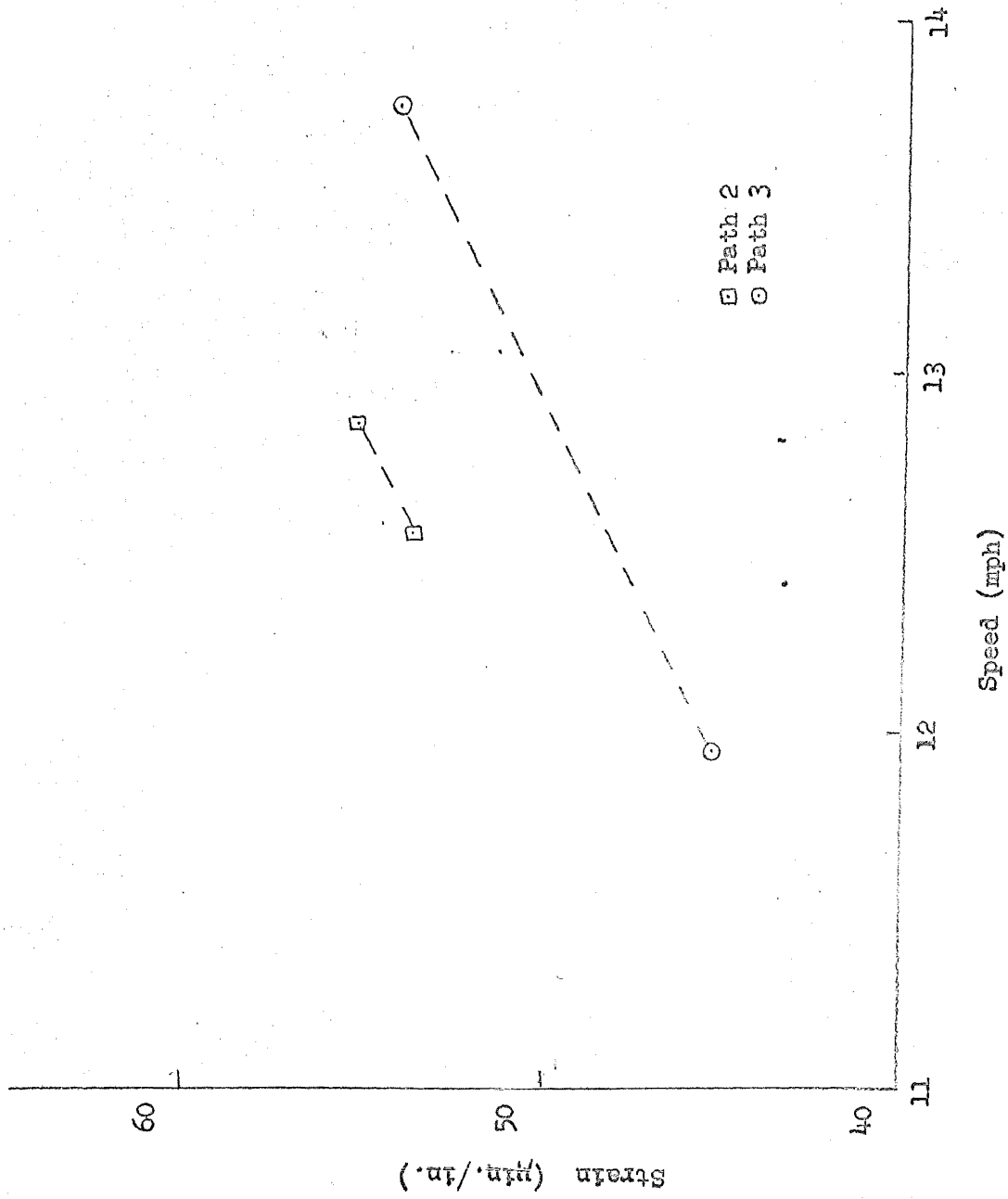


Fig. 8 Beam 2 Bottom Surface Peak Strains; Impact Runs

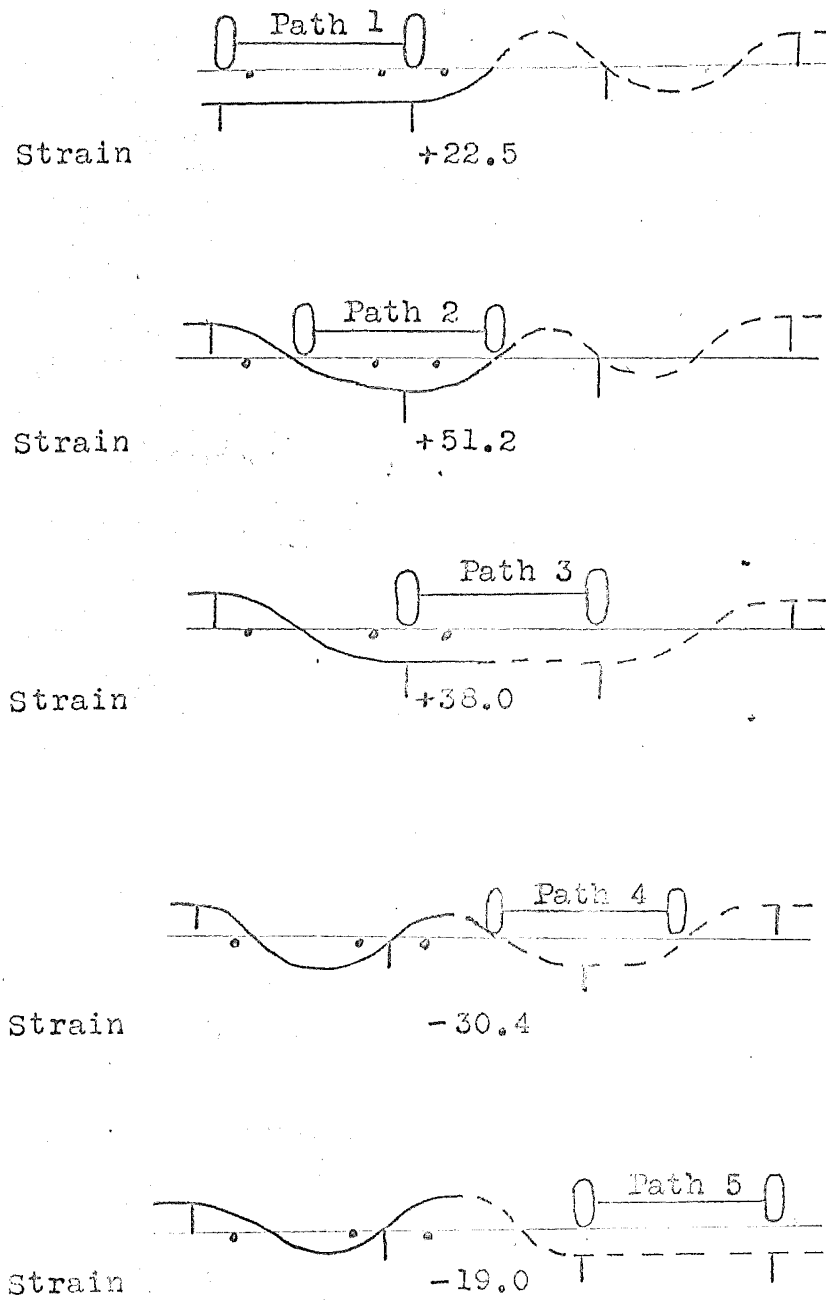


Fig. 9 Peak Deck Slab Transverse Strains

(Microinches per Inch)

Compressive Strains Shown Negative

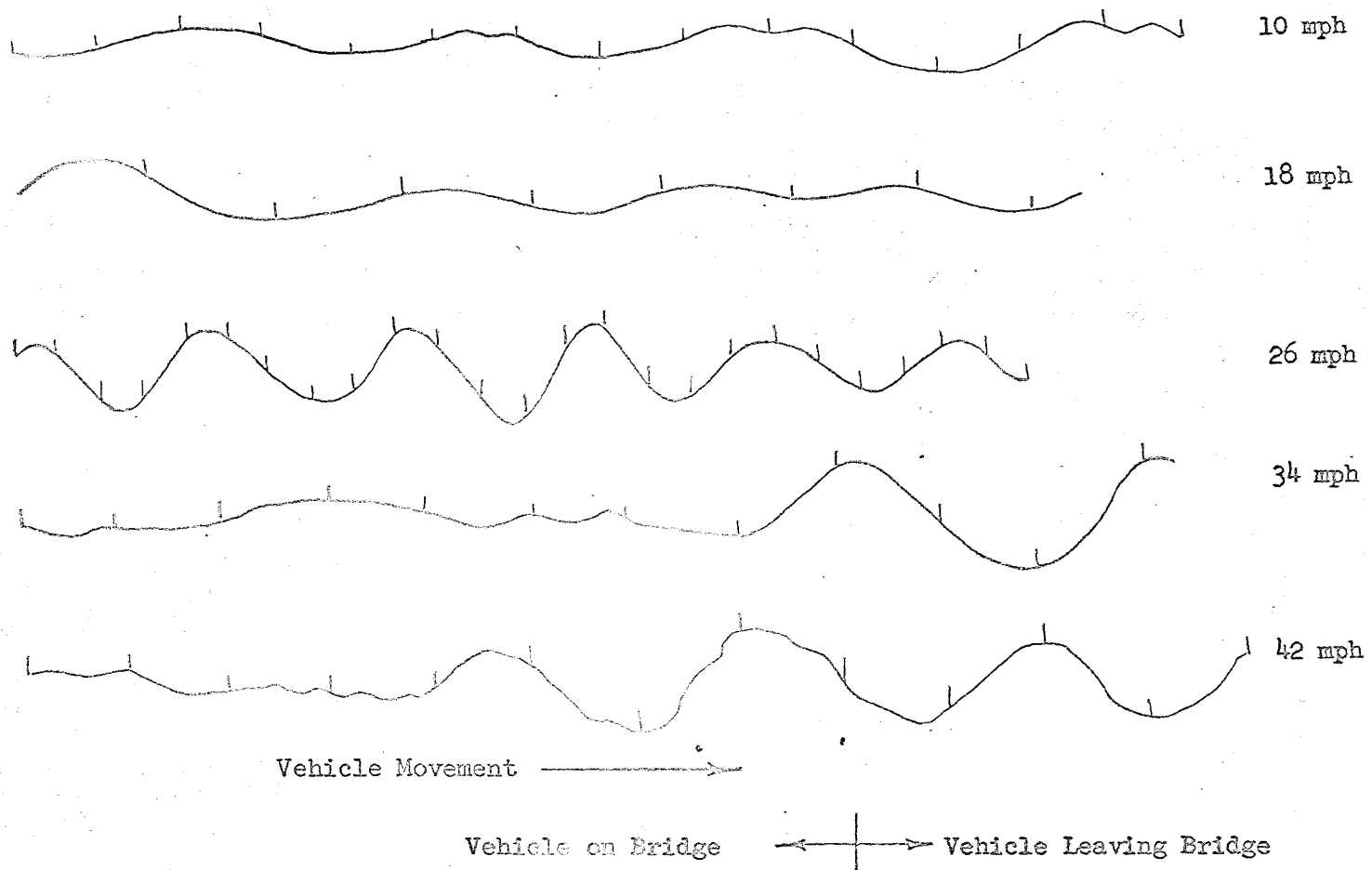


Fig. 10 Typical Test Vehicle Records
 (0.1 second time intervals shown as ticks)

9. A C K N O W L E D G E M E N T S

This report stems from a field study undertaken as a cooperative research project by the U. S. Bureau of Public Roads and the Lehigh University Department of Civil Engineering acting for the Pennsylvania Department of Highways.

Professor David A. VanHorn, Chairman of the Structural Concrete Division of the Department of Civil Engineering, Lehigh University, planned and supervised the conduct of the research for the University. Staff members and research assistants who ably assisted in the field work included Messrs. A. A. Guilford, W. Douglas, T. W. Schaffer, and R. Dietz. Mr. Guilford and Mr. Schaffer are presently working on a companion report to this which will analyze the static live load experimental data. The Bureau of Public Roads Task Group for Bridge Research consisted of Messrs. C. A. Ballinger, W. L. Armstrong, H. R. Laatz, and the author.

Professor VanHorn has also acted as the author's faculty advisor for this study. His keen interest in guiding the preparation of this report is sincerely appreciated.

10. REFERENCES

1. Pennsylvania Department of Highways
STANDARDS FOR PRESTRESSED CONCRETE BRIDGES
S-3900 to S-3909 1959, 1960 and 1962.
2. American Association of State Highway Officials
STANDARD SPECIFICATIONS FOR HIGHWAY BRIDGES, 1957.
3. Varney, R. F.
DYNAMIC TESTS ON A ROLLED-BEAM
COMPOSITE SIMPLE SPAN BRIDGE
South Dakota Department of Highways, 1963.
4. Kinnier, H. L., McKeel, W. T.
A DYNAMIC STRESS STUDY OF THE
HAZEL RIVER BRIDGE
Virginia Council of Highway Investigation
and Research, 1965.
5. Rosli, A.
THE DYNAMIC BEHAVIOUR OF PRESTRESSED
BRIDGES
Cement and Concrete Association (London)
Translation of a paper presented at the
Sixth Congress of the International
Association for Bridge and Structural
Engineering at Stockholm, 1960.
6. Reilly, R. J., Looney, C. T. G.
DYNAMIC BEHAVIOR OF HIGHWAY BRIDGES
Department of Civil Engineering
University of Maryland, 1966.
7. The Preload Co. Inc.
CLASSIFICATION OF PRESTRESSED CONCRETE
BRIDGES IN THE UNITED STATES AND WESTERN
EUROPE
A report for the Corps of Engineers, U. S.
Army, Engineer Research and Development
Laboratories, 1958.
8. Slepetz, John M.
A STUDY OF THE DYNAMIC RESPONSE OF
HIGHWAY STRINGER BRIDGES BY MECHANICAL
IMPEDANCE-MOBILITY METHODS
M. S. Thesis
University of Virginia, 1962.

11. B I B L I O G R A P H Y

1. Varney, R. F., Galambos, C. F.
FIELD DYNAMIC LOADING STUDIES OF HIGHWAY
BRIDGES IN THE U. S.; 1948-1965
HRB Highway Research Record Number 76, 1965.
This compilation contains bridge descriptions
and references to 22 publications.
2. Bouwkamp, J. G., Brown, C. B., Scheffey, C. F.,
Yaghmai, S.
BEHAVIOR OF A SINGLE SPAN COMPOSITE GIRDER
BRIDGE
University of California, Berkeley, 1965.
3. Bouwkamp, J. G.
BEHAVIOR OF A SKEW STEEL DECK BRIDGE UNDER
STATIC AND DYNAMIC LOADS
University of California, Berkeley, 1965.
4. Davis, R. E., Kozak, J. J., Scheffey, C. F.
STRUCTURAL BEHAVIOR OF A BOX GIRDER BRIDGE
California Division of Highways, Bridge
Department, 1965.
5. Hyde, D.
DYNAMIC TESTS ON A ROLLED-BEAM COMPOSITE
CONTINUOUS SPAN BRIDGE
South Dakota Department of Highways, 1963
6. Kinnier, H.L., McKeel, W. T.
A DYNAMIC STRESS STUDY OF THE HAZEL RIVER
BRIDGE
Virginia Council of Highway Investigation and
Research, 1964.
7. Kinnier, H. L., McKeel, W. T.
A DYNAMIC STRESS STUDY OF THE ALUMINUM BRIDGE
OVER THE APPOMATTOX RIVER AT PETERSBURG
Virginia Council of Highway Investigation
and Research, 1965.
8. Newton, J. G., Walker, L. G.
EXPERIMENTAL USE OF HIGH-STRENGTH REINFORCING
STEEL
Bridge Division, Texas Highway Department, 1966.

9. Reilly, R. J., Looney, C. T. G.
DYNAMIC BEHAVIOR OF HIGHWAY BRIDGES
Department of Civil Engineering
University of Maryland, 1966.
10. Varney, R. F.
DYNAMIC TESTS ON A ROLLED-BEAM COMPOSITE
SIMPLE SPAN BRIDGE
South Dakota Department of Highways, 1963.
11. Welden, N.
LIVE LOAD DEFLECTIONS IN A PRESTRESSED STEEL
BRIDGE
AISC Engineering Journal, January 1965.